New physics searches with heavy-ion collisions at the LHC

Roderik Bruce[1], David d'Enterria*[2], Albert de Roeck[2], Marco Drewes[3], Glennys R. Farrar[4], Andrea Giammanco[3], Oliver Gould[5], Jan Hajer[3], Lucian Harland-Lang[6], Jan Heisig[3], John M. Jowett[1], Sonia Kabana[7], Georgios K. Krintiras[3], Michael Korsmeier[8,9,10], Michele Lucente[3], Guilherme Milhano[11,12], Swagata Mukherjee[13], Jeremi Niedziela[2], Vitalii A. Okorokov[14], Arttu Rajantie[15], and Michaela Schaumann[1]

[1]CERN, BE Department, CH-1211 Geneva, Switzerland
[2]CERN, EP Department, CH-1211 Geneva, Switzerland
[3]Centre for Cosmology, Particle Physics and Phenomenology, Université catholique de Louvain, B-1348 Louvain-la-Neuve, Belgium
[4]Centre for Cosmology and Particle Physics, New York University, NY, NY 10003, USA
[5]Helsinki Institute of Physics, University of Helsinki, FI-00014, Finland
[6]Rudolf Peierls Centre, Beecroft Building, Parks Road, Oxford, OX1 3PU, UK
[7]Department of Physics, University of Nantes, and SUBATECH, 4 rue Alfred Kastler, 44307 Nantes, France
[8]Institute for Theoretical Particle Physics and Cosmology, RWTH Aachen University, Aachen, Germany
[9]Dipartimento di Fisica, Università di Torino, Torino, Italy
[10]Istituto Nazionale di Fisica Nucleare, Sezione di Torino, Torino, Italy
[11]LIP, Av. Prof. Gama Pinto, 2, P-1649-003 Lisboa, Portugal
[12]Instituto Superior Técnico, Universidade de Lisboa, Av. Rovisco Pais 1, 1049-001, Lisboa, Portugal
[13]III. Physikalisches Institut A, RWTH Aachen University, Aachen, Germany
[14]National Research Nuclear University MEPhI, Moscow, Russia
[15]Department of Physics, Imperial College London, London SW7 2AZ, UK

December 18, 2018

Abstract

This document summarizes proposed searches for new physics accessible in the heavy-ion mode at the LHC, both through hadronic and ultraperipheral $\gamma\gamma$ interactions, and that have a competitive or, even, unique discovery potential compared to standard proton-proton collision studies. Illustrative examples include searches of new particles — such as axion-like pseudoscalars, radions, magnetic monopoles, new long-lived particles, dark photons, and sexaquarks as dark matter candidates — as well as new interactions, such as non-linear or non-commutative QED extensions. We argue that such interesting possibilities constitute a well-justified scientific motivation, complementing standard quark-gluon-plasma physics studies, to continue running with ions at the LHC after the Run-4, i.e. beyond 2030, including light and intermediate-mass species, accumulating nucleon-nucleon integrated luminosities in the accessible fb^{-1} range per month.

*E-mail contact person for EPPS: dde@cern.ch

1 Introduction

Physics beyond the Standard Model (BSM) is necessary in order to explain numerous unsolved empirical and theoretical problems in high energy physics. Prominent examples among them are the nature of dark matter (DM), the origin of matter-antimatter asymmetry (baryogenesis), and finite neutrino masses, on the one hand, as well as the Higgs mass fine-tuning, the null $\theta_{\rm QCD}$ Charge-Parity (CP) violation term in Quantum Chromodynamics (QCD), the origin of fermion families and mixings, charge quantization, the cosmological constant, and a consistent description of quantum gravity, on the other hand. Most solutions to these problems require new particles — such as supersymmetric partners, dark photons, right-handed neutrinos, axions, monopoles — and/or new interactions, which have so far evaded observation due to their large masses and/or their small couplings to SM particles. Two common complementary routes are followed at colliders in order to search for BSM physics. If BSM appears at high masses, one needs to maximize the center-of-mass (c.m.) energy $\sqrt{s}$. If BSM involves small couplings, one needs to maximize the luminosity $\mathcal{L}$. At face value, both strategies present obvious drawbacks for searches in heavy-ions (HI) compared to *pp* collisions at the LHC: (i) PbPb collisions run at roughly 2.5 times lower nucleon-nucleon c.m. energies than *pp* collisions ($\sqrt{s_{\rm NN}} = 5.5$ vs. 14 TeV), and (ii) the nucleon-nucleon luminosities are about a factor 100 smaller ($\mathcal{L}_{\rm NN} = A^2 \times 6 \cdot 10^{27}\,{\rm cm}^{-1}{\rm s}^{-2} = 2.5 \cdot 10^{32}\,{\rm cm}^{-2}{\rm s}^{-1}$ for PbPb vs. $\mathcal{L}_{\rm pp} = 2 \cdot 10^{34}\,{\rm cm}^{-2}{\rm s}^{-1}$).

During the HL-LHC phase, whose main focus are BSM searches, the luminosity of *pp* collisions will be maximized, inevitably leading to a large number of overlapping collisions per bunch crossing (pileup). Pileup translates into a rising difficulty to record all interesting *pp* events, and thereby an unavoidable increase of the kinematical thresholds for triggers and reconstruction objects in order to reduce unwanted backgrounds. Pileup also leads to an intrinsic complication in the reconstruction of exclusive final-states (in particular neutral ones, such as $X \to \gamma\gamma$ at not too high masses) and of displaced vertices from e.g. long-lived-particles (LLPs) that appear in many BSM scenarios. In this context, if BSM has low couplings with the SM and is "hiding well" at relatively low masses with moderately "soft" final states, HI collisions — with zero pileup, optimal primary vertexing (thanks to the large number of primary tracks), reduced trigger thresholds (down to zero p_T, in some cases), plus unique and "clean" $\gamma\gamma$ exclusive final-states in ultraperipheral interactions with luminosities enhanced by factors of order $\mathcal{L}_{\rm PbPb}(\gamma\gamma)/\mathcal{L}_{pp}(\gamma\gamma) = Z^4 \times \mathcal{L}_{\rm PbPb}/\mathcal{L}_{pp} = 4.5 \cdot 10^7 \times (6 \cdot 10^{27})/(2 \cdot 10^{34}) \approx 10$ — present clear advantages compared to *pp*.

The purpose of this document is to summarize various BSM search possibilities accessible at the LHC in the HI mode, and thereby provide novel arguments to prolong the HI programme beyond the LHC Run-4. New physics searches that are competitive (or, at least, complementary) with *pp* studies at the LHC are listed in Table 1, and succinctly presented hereafter. This list is not comprehensive, but is representative of the type of processes that are attractive and possible with ions from the perspective of new-physics searches. After a summary of the LHC heavy-ion performance of current and future runs (Section 2), the document is organized along the following four BSM production mechanisms:

1) Ultraperipheral $\gamma\gamma$ collisions (UPCs), producing, e.g. axion-like particles (ALPs), Section 3.
2) "Schwinger" production through strong classical EM fields, producing, e.g. monopoles, Section 4.
3) Hard scattering processes, producing, e.g. displaced signals from new LLPs, Section 5.
4) Thermal production in the quark-gluon-plasma (QGP), producing, e.g. sexaquarks, Section 6.

Processes 1), 2), and 4) explicitly use a BSM production mechanism that is unique (or significantly enhanced compared to the *pp* mode) in HI collisions, whereas in processes of the type 3), it is the comparatively reduced pileup backgrounds that renders HI collisions interesting.

2 Accelerator considerations

The nominal LHC operation includes HI collisions roughly during 1 month every year, but even accounting with such roughly $\times 10$ lower integrated running time than *pp*, several BSM searches appear more competitive with ions than with protons as shown below. The performance of the HI runs up until the end of Run-2 has been very good, reaching instantaneous PbPb luminosities 6 times higher than the design value of $10^{27}\,{\rm cm}^{-1}{\rm s}^{-2}$ (equivalent to a nucleon-nucleon luminosity of $\mathcal{L}_{\rm NN} = 2.5 \cdot 10^{32}\,{\rm cm}^{-2}{\rm s}^{-1}$). Four LHC experiments are now taking data with HI collisions, and physics runs have also been carried out with

Production mode	BSM particle/interaction	Remarks
Ultraperipheral	Axion-like particles	$\gamma\gamma \to a$, $m_a \approx 0.5$–$100\,\text{GeV}$
	Radion	$\gamma\gamma \to \phi$, $m_\phi \approx 0.5$–$100\,\text{GeV}$
	Born-Infeld QED	via $\gamma\gamma \to \gamma\gamma$ anomalies
	Non-commutative interactions	via $\gamma\gamma \to \gamma\gamma$ anomalies
Schwinger process	Magnetic monopole	Only viable in HI collisions
Hard scattering	Dark photon	$m_{A'} \lesssim 1\,\text{GeV}$, advanced particle ID
	Long-lived particles (heavy ν)	$m_{\text{LLP}} \lesssim 10\,\text{GeV}$, improved vertexing
Thermal QCD	Sexaquarks	DM candidate

Table 1: Examples of new-physics particles and interactions accessible in searches with HI collisions at the LHC, listed by production mechanism. Indicative competitive mass ranges and/or the associated measurement advantages compared to the *pp* running mode are given.

a novel mode of operation with *p*Pb collisions that was not initially foreseen. The excellent performance was made possible through many improvements in the LHC and the injector chain. In particular, the average colliding bunch intensity in 2018 was up to about $2.3 \cdot 10^8$ Pb/bunch, which is more than 3 times higher than the LHC design value. For the next PbPb run in 2021, it is planned to further increase the total LHC intensity through a decrease of bunch spacing to 50 ns, in order to fit 1 232 bunches in the LHC. A further increase of the injected intensity seems difficult without additional hardware [1]. In the LHC, any increase of ion luminosity is ultimately limited by the risk of quenching magnets, either by secondary beams with the wrong magnetic rigidity created in the collisions [2–6] or by leakage from the halo cleaning by the collimators [7–9]. As a mitigation, it is planned to install additional collimators in the next long shutdown of the LHC (2019–2020) to allow higher luminosity and intensity [10–12]. Using the predicted beam and machine configuration, the future luminosity performance has been estimated for PbPb and *p*Pb [13]. During a 1-month run, assuming that the instantaneous luminosity is leveled at the current values around $6 \cdot 10^{27}\,\text{cm}^{-2}\text{s}^{-1}$, the integrated luminosity per experiment is estimated to $3.1\,\text{nb}^{-1}$ for PbPb and $700\,\text{nb}^{-1}$ for *p*Pb (without levelling), equivalent to NN luminosities of $\mathcal{L}_{\text{NN}} \approx 0.15\,\text{fb}^{-1}$.

In the presently approved CERN planning, it is foreseen to perform another four and a half PbPb runs before the end of LHC Run-4 in 2029, accumulating $\sim 13\,\text{nb}^{-1}$ in total. Furthermore, one short *p*Pb run is planned, as well as one reference *pp* run. No further HI runs have so far been planned after Run-4. These plans are detrimental for the full exploitation of the BSM possibilities opened in HI collisions, that require as large integrated luminosities as possible. A revised proposal for Runs-3 and 4 and plans to extend the LHC nuclear programme beyond Run-4 have been formulated [13]. The BSM physics possibilities summarized here, complement and reinforce that scientific case. These studies involve more time spent on *p*Pb runs and also collisions of lighter nuclei, e.g. Ar, O, or Kr [13, 14]. As shown in Table 2, the latter have the potential to reach $\times$(2–15) higher NN luminosities, which would benefit any BSM search based on hard-scattering processes (Section 5), although the corresponding $\gamma\gamma$ luminosities (Section 3) would be reduced by a $(Z_{\text{PbPb}}/Z_{\text{AA}})^4$ factor. The estimated parameters for a range of lighter ions rely on the assumption that the achievable bunch intensity N_b for a nucleus with charge number Z and mass number A can be scaled from the Pb bunch intensity as $N_b(Z, A) = N_b(82, 208) \times (Z/82)^p$, where the power $p = 1.5$ is estimated from previous experience of nuclear beams for the CERN fixed-target experiments and the short run with Xe in the LHC in 2017 [15]. It should be noted that these estimates carry a significant uncertainty, since no attempts have been made experimentally at optimizing these beams for the LHC. Furthermore, the integrated luminosity per month in Table 2 has been calculated using a simplified model, which gives slightly more optimistic values for Pb than the $3.1\,\text{nb}^{-1}$ stated above, which was simulated with a more detailed and accurate model. Total integrated luminosities in the range 0.2–$3\,\text{fb}^{-1}$ are expected depending on the ion-ion colliding system. We stress that, if BSM or other physics cases eventually justify it, one can consider running a full "*pp* year" with ions at the LHC, leading to roughly factors of $\times 10$ larger integrated luminosities than those listed in Table 2.

		$^{16}_{8}$O	$^{40}_{18}$Ar	$^{40}_{20}$Ca	$^{78}_{36}$Kr	$^{129}_{54}$Xe	$^{208}_{82}$Pb
γ	$[10^3]$	3.76	3.39	3.76	3.47	3.15	2.96
$\sqrt{s_{\rm NN}}$	[TeV]	7	6.3	7	6.46	5.86	5.52
$\sigma_{\rm had}$	[b]	1.41	2.6	2.6	4.06	5.67	7.8
N_b	$[10^9]$	6.24	1.85	1.58	0.653	0.356	0.19
ϵ_n	$[\mu$m]	2	1.8	2	1.85	1.67	1.58
Z^4	$[10^6]$	$4.1 \cdot 10^{-3}$	0.01	0.16	1.7	8.5	45
$\widehat{\mathcal{L}}_{\rm AA}$	$[10^{30}\,{\rm cm}^{-2}{\rm s}^{-1}]$	14.6	1.29	0.938	0.161	0.0476	0.0136
$\widehat{\mathcal{L}}_{\rm NN}$	$[10^{33}\,{\rm cm}^{-2}{\rm s}^{-1}]$	3.75	2.06	1.5	0.979	0.793	0.588
$\langle\mathcal{L}_{\rm AA}\rangle$	$[10^{27}\,{\rm cm}^{-2}{\rm s}^{-1}]$	8990	834	617	94.6	22.3	3.8
$\langle\mathcal{L}_{\rm NN}\rangle$	$[10^{33}\,{\rm cm}^{-2}{\rm s}^{-1}]$	2.3	1.33	0.987	0.576	0.371	0.164
$\int_{\rm month}\mathcal{L}_{\rm AA}{\rm d}t$	$[{\rm nb}^{-1}]$	$1.17 \cdot 10^4$	1080	799	123	28.9	4.92
$\int_{\rm month}\mathcal{L}_{\rm NN}{\rm d}t$	$[{\rm fb}^{-1}]$	2.98	1.73	1.28	0.746	0.480	0.210

Table 2: LHC beam parameters and performance for collisions from O up to Pb ions, with a moderately optimistic value of the scaling parameter $p = 1.5$ introduced in [13, 14]. Here $\sigma_{\rm had}$ is the hadronic cross section, ϵ_n the normalized emittance, and the Z^4 factor is provided to indicate the order-of-magnitude enhancement in $\gamma\gamma$ cross sections expected in UPCs compared to pp collisions Nucleus-nucleus (AA) and nucleon-nucleon (NN) luminosities $\mathcal{L}$ are given at the start of a fill, $\widehat{\mathcal{L}}$, and as time averages, $\langle\mathcal{L}\rangle$, with typical assumptions used to project future LHC performance. Total integrated luminosities in typical 1-month LHC runs are given in the last two rows.

3 Ultraperipheral $\gamma\gamma$ collisions

In HI collisions, the highly relativistic ions act as a strong source of electromagnetic (EM) radiation, enhanced by the large proton charge number Z. This offers a natural environment in which to observe the photon-initiated production of BSM states with QED couplings. The cross section for the $\gamma\gamma$ production of any particle X can be calculated within the equivalent photon approximation [16] as

$$\sigma_{A_1A_2\to A_1XA_2} = \int {\rm d}x_1{\rm d}x_2\, n(x_1)n(x_2)\widehat{\sigma}_{\gamma\gamma\to X} = \int {\rm d}m_{\gamma\gamma}\, \frac{{\rm d}\mathcal{L}_{\rm eff}}{{\rm d}m_{\gamma\gamma}}\widehat{\sigma}_{\gamma\gamma\to X}\ , \tag{1}$$

where x_i is the longitudinal momentum fraction of the photon emitted by ion A_i. This factorizes the result in terms of a $\gamma\gamma \to X$ subprocess cross section $\widehat{\sigma}$ of a (BSM) system X, and fluxes $n(x_i)$ of photons emitted by the ions. The latter are precisely determined in terms of the ion EM form factors, and are in particular enhanced by $\propto Z^2$ for each ion, leading to an overall $\sim Z^4$ enhanced production in ion-ion collisions ($\sim 5 \cdot 10^7$ for PbPb). The experimental signal of UPC processes is very clean with the system X and nothing else produced in the central detector. Moreover, since the virtuality of the emitted photons is restricted to be very small $Q^2 \sim 1/R_A^2$, where R_A is the ion radius, the X object is produced almost at rest [17]. The impact parameters $b_\perp$ of UPCs with ions, with $b_\perp \gg 2R_A$ beyond the range of additional strong interactions, are significantly larger than in the pp case, and the associated gap survival probability is also significantly bigger than for EM proton interactions. This effect can be accounted for precisely and enters at the $\mathcal{O}(10\,\%)$ level in terms of corrections to $\gamma\gamma$ interactions, with rather small uncertainties [18]. In addition, the background from QCD-initiated production is essentially completely removed by the requirement that the system X and nothing else is seen in the central detector [18].

A wide program of photon-photon measurements and theoretical work is ongoing in the context of pp collisions at the LHC [21], with dedicated proton taggers (Roman Pots, RP) installed inside the LHC tunnel at ∼220 meters from the ATLAS [22] and CMS [23] interaction points. In comparison to the pp mode, UPCs with HI offer the distinct advantage of studying such photon-fusion processes in an environment where pileup is absent, forward tagging is unnecessary, and considerably lower masses can be probed. Indeed, two-photon processes in pp collisions at high luminosity can only be observed by tagging the forward protons inside the LHC tunnel with geometrical acceptances that bound any central system to have, at least, $m_X \gtrsim 100\,{\rm GeV}$. Figure 1 compares the effective $\gamma\gamma$ luminosity as a function of $m_{\gamma\gamma}$, defined in cross section (1), for pp and PbPb collisions at their nominal c.m. energies and

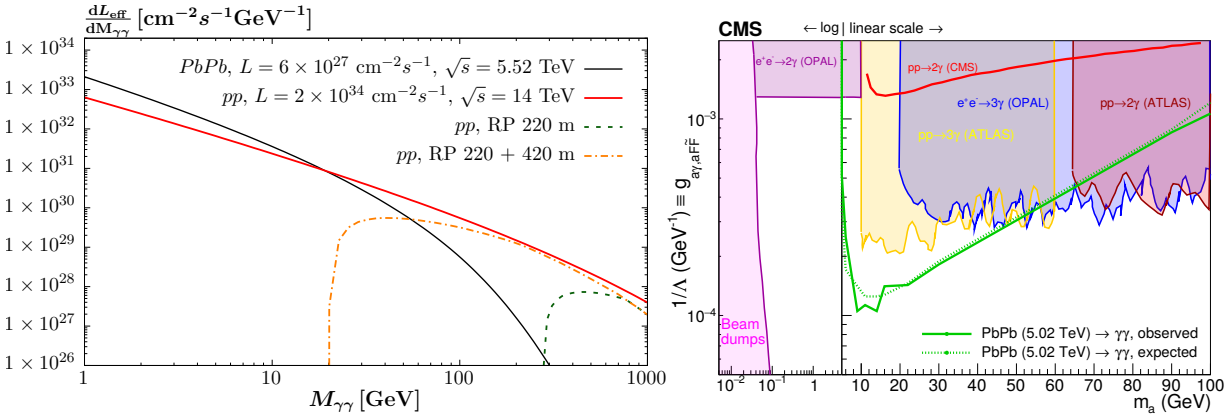

Figure 1: Left: Effective $\gamma\gamma$ luminosity vs. photon-fusion mass in PbPb and pp collisions at the LHC. In the pp case, the (actually "usable") $\gamma\gamma$ luminosity is also shown with proton tagging at 220 m (currently installed) and 420 m (proposed). Right: Current 95% CL exclusion limits in the ALP-γ coupling vs. ALP mass plane [19, 20].

instantaneous luminosities. Even after accounting for the reduced beam luminosity in PbPb collisions, the effective $\gamma\gamma$ luminosity is a factor of two higher in PbPb than the (purely theoretical) pp values at low masses. As a matter of fact, taking into account the acceptance in the proton fractional momentum loss ξ of the RP detectors at 220 m ($0.02 < \xi < 0.15$) [22, 23] and even including proposed RPs at 420 m ($0.0015 < \xi < 0.15$) [24], only PbPb enables studies in the region below $m_X \approx 100$ GeV. Running pp at low pileup would cover the low mass region albeit with significantly reduced $\gamma\gamma$ luminosities. Various $\gamma\gamma$ BSM processes are available in the SuperChic [18] and STARlight [25] Monte Carlo generators.

3.1 Axion-like particles

Axion-like particles (ALPs) constitute a class of pseudoscalars with couplings to SM fermions or gauge bosons through dimension-five operators. In some cases they may be Goldstone bosons of an approximate, spontaneously broken, global symmetry. In this sense they are inspired by original axions arising from the Peccei-Quinn mechanism to solve the absence of CP violation in QCD [26, 27], but in general they do not have to solve the strong CP problem, and are therefore to be understood as purely phenomenological extensions of the Standard Model. An ALP couples to photons through the operator $\mathscr{L} \supset \frac{a}{4f} F_{\mu\nu}\tilde{F}^{\mu\nu}$, where f is the decay constant of the ALP. They can be produced through photon-fusion $\gamma\gamma \to a$ or associated $f\bar{f} \to \gamma a$ production, where the latter tends to be the strongest production mode at electron or proton machines. In the mass range below about 100 GeV, photon fusion in ultraperipheral HI collisions is competitive thanks to the huge Z^4 enhancement in the photon luminosity [19].

A second key feature is that the only SM background is light-by-light (LbL) scattering, which is notoriously tiny [28]. This means that it is crucial that the Lagrangian $\mathscr{L}$ above provides the dominant coupling of the ALP to the SM: Any competing branching ratios to leptons or jets would degrade the reach, as the backgrounds in those final states are unsupressed. Evidence for LbL scattering in PbPb UPCs has been reported by ATLAS [29] and CMS [20]. The latter one also provides the best current limits on ALPs in the mass range from $m_a = 5$ to 50 GeV for coupling to photons only (Fig. 1 right), and $m_a = 5$ to 10 GeV for a scenario with hypercharge coupling as well. For a recast of the ATLAS data to a limit on ALPS, see [13, 30]. Given that the higher mass ALPs will be well covered by the regular pp runs, PbPb collisions will likely remain the only choice when searching for ALPs up to $m_a \approx 100$ GeV, though a comparison of the higher-mass reach for lighter ions would be interesting. Going below $m_a < 5$ GeV is not possible for ATLAS and CMS, due to trigger and noise limitations in the calorimeters, but the range $m_a \approx 0.5$–5 GeV can be covered by UPC measurements in ALICE and LHCb, complementing a mass range that Belle II is also expected to measure reasonably well [31]. Finally, as more data is gathered, the LbL background will become a limitation. The limits would therefore benefit substantially if the diphoton invariant mass resolution could be improved, possibly by making use of γ conversions.

3.2 Born-Infeld non-linear QED, non-commutative QED

The possibility of non-linear Born-Infeld extensions of QED has a long history, first proposed in the 1930s [32], they appear naturally in string-theory models [33]. However, remarkably the limit on the mass scale of such extensions has until recently been at most at the level of 100 MeV [34]. The first LHC measurement of LbL scattering in HI collisions [29] has enabled to extend the upper limit of non-linear QED modifications by 3 orders of magnitude, up to scales $\Lambda_{\rm BI} \gtrsim 100\,\text{GeV}$, which in turn imposes a lower limit of 11 TeV on the magnetic monopole mass in the case of a BI extension of the SM in which the $\text{U}(1)_Y$ hypercharge gauge symmetry is realized non-linearly [34]. Future LbL measurements in HI UPCs will offer the possibility to further probe Born-Infeld and other non-linear extensions of QED.

Non-commutative (NC) geometries also naturally appear within the context of string/M-theory [35]. One consequence of this possibility is that QED takes on a non-Abelian nature due to the introduction of 3- and 4-point functions, leading to observable signatures in the total and differential cross sections of QED processes. In [36] it has been demonstrated that non-commutative effects impact $\gamma\gamma \to \gamma\gamma$ scattering at tree-level, and that a study of its differential cross sections at a photon-collider in the few hundred of GeV range can bound non-commutative scales of order a TeV. Somehow lower limits can be reached through the detailed study of the LbL process accessible in UPCs with ions at the LHC.

3.3 Other BSM particles

There are several other possible BSM signals that couple to a pair of photons. It has been argued e.g. that $\gamma\gamma \to \gamma\gamma$ collisions can be used to search for radions [37], gravitons [38, 39] and unparticles [40]. The UPC signatures would be resonances and/or a non-trivial interference pattern of these new contributions with the SM LbL background. The scalar radion would behave identically as the pseudoscalar ALP example discussed in Section 3.1. Evaluating the search potential requires dedicated studies, in particular to compare with the reach of other studies sensitive to these models, such as the mono-photon searches in standard *pp* collisions. In the case of unparticles, unitarity and bootstrap bounds must be accounted for as well [41–43].

Charged supersymmetric (SUSY) particles like sleptons and charginos are also natural targets for $\gamma\gamma$ collisions, especially in the squeezed regime where the standard lepton-plus-missing-E_T searches lose sensitivity. Unfortunately, the existing limits from LEP already exclude the parameter space, in simplified SUSY scenarios, which is accessible to HI collisions. It may however be possible to extract a competitive limit with $\gamma\gamma$ collisions from the proton beams [44, 45].

Magnetic monopoles necessarily couple strongly to photons [46]. Hence it has been suggested that $\gamma\gamma$ collisions are a natural candidate for monopole searches, either by direct detection [47–50], by the formation of monopolium bound-states [48, 49, 51] or via the contribution of virtual monopole loops to LbL scattering [52–54]. However, these approaches have been criticized for their reliance on perturbative loop expansions in the strong monopole coupling [55, 56]. Such limitations are circumvented in the production mechanism from classical EM fields discussed next.

4 Strong electromagnetic fields

4.1 Magnetic monopoles

There are compelling theoretical reasons for the existence of magnetic monopoles [46, 57, 58], such as providing a mechanism to explain charge quantization in the SM. Consequently, there have been many searches [59], including currently a dedicated LHC experiment, MoEDAL [60]. Due to the Dirac quantization condition, magnetic monopoles are necessarily strongly coupled, hence perturbative loop expansions for their cross sections cannot be trusted. In fact, it has been argued that the pair production cross section of semiclassical monopoles [61, 62] in *pp* or elementary particle collisions suffers from an enormous non-perturbative suppression [63–65], $\sigma_{M\overline{M}} \propto \text{e}^{-4/\alpha} = 10^{-238}$, independent of collision energy. It is not known if the same suppression applies to point-like elementary monopoles, but if it does [66], it implies that magnetic monopoles cannot realistically be produced in *pp* collisions, irrespective of the energy and luminosity of the collider. The assumptions that led to the exponential cross section suppression do

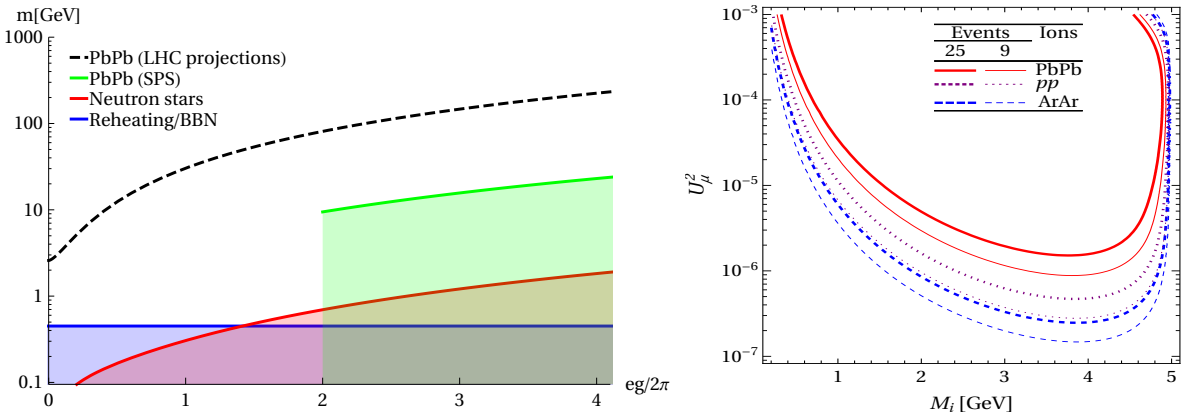

Figure 2: Left: Lower bounds for the magnetic monopole mass vs. units of magnetic charge [70]. Right: Estimated CMS reach for heavy neutrinos, with mass M_i and muon-neutrino mixing angle U_μ, from B-meson decays in pp, ArAr, and PbPb collisions with equal running time [71].

not apply to HI collisions due to the non-perturbatively large magnetic fields that are produced, which are strongest in UPCs [67]. These fields may produce magnetic monopoles by the electromagnetic dual of Schwinger pair production [68], the calculation of which does not rely on perturbative expansions in the coupling. To date, there has only been one search for magnetic monopoles in HI collisions, conducted at SPS [69], which has led to the strongest bounds on their mass [70]. Searches in HI collisions at the LHC could in principle produce 2–3 orders of magnitude heavier monopoles, directly testing their existence in the hundreds of GeV mass range for the first time (Fig. 2 left).

From the experimental point of view, triggering and tracking constitute challenges for the LHC experiments. Magnetic monopoles would manifest as highly ionizing particles, and their trajectories in a uniform magnetic field are parabolic. These are striking features that, on the one hand, help to reject background events to very small levels and, on the other, may cause monopoles to be missed by standard reconstruction algorithms, as a basic assumption of charged-particle tracking is that particle trajectories are helical. Given that their production by strong magnetic fields is most likely in UPCs, the usual UPC signature of an almost empty detector would be exploitable to select monopole events. Alternatively a monopole search can be carried out using passive trapping detectors, exploiting the absolute stability of monopoles as used in the MoEDAL experiment, during the HI running mode. Unlike active detectors, this method gives no direct information about the process that produced the monopole, but it has the advantage that there is no SM background and therefore no risk of a false positive event.

5 Hard scattering processes

5.1 Long-lived particles

Many BSM models predict the existence of *long lived particles* (LLPs) that can travel macroscopic distances after being produced, cf. e.g. [72]. Their existence is in many cases linked to the solution of fundamental problems in particle physics and cosmology, such as the origin of neutrino masses, the DM puzzle, or baryogenesis. The LLPs usually owe their longevity to a (comparably) light mass, a feeble coupling to ordinary matter, or a combination of both. If such particles are produced in HI collision, the feeble interaction allows most of them to leave the quark-gluon plasma unharmed. Due to the long lifetime, the tracks from their decay into SM particles can easily be distinguished from the large number of tracks that originate from the collision point (a single one, given the absence of pileup when running in the HI mode). Hence, HI collisions can potentially provide a cleaner environment for LLP searches than pp. The main obstacle is the considerably lower luminosity in HI compared to proton runs, which means that the total number of LLPs produced in the former is always much smaller than in the latter. However, there are at least two factors that can make the observable number of LLP events competitive [71].

First, due to the absence of pileup, the probability of misidentifying the primary vertex is practically negligible for HI collisions because all tracks originate from a small (fm sized) region. This is in contrast to the HL-LHC pileup with proton beams, which leads to a comparable number of tracks as a single PbPb collision [73, 74] originating from different points in the same bunch crossing and thereby creating a considerable combinatorial track background for displaced signatures. HI collisions entirely remove the problem of identifying the location of the primary vertex, which may be the key to trespass the "systematics wall" due to uncertainties in cases where background contamination mostly comes from real SM particles (as opposed to misidentified or fake ones). Although a large track multiplicity is expected to degrade the reconstruction and identification of displaced vertices, the adverse effect of pileup on vertex-finding performance is coming more from the presence of additional primary-interaction vertices than from the sheer number of tracks, as demonstrated by the better b-quark tagging performance in pPb compared to pp collisions in $t\bar{t}$ studies [75].

Second, absence of pileup allows to operate the detectors with minimal (zero bias) triggers. This is, e.g., an advantage in scenarios in which LLPs lead to low-p_T final states. In [71] it has been shown that this can make searches for typical LLP signatures such as from heavy neutrinos, competitive in HI collisions. Heavy ν's with masses of a few GeV could simultaneously explain the masses of the SM neutrinos and the baryon asymmetry of the universe [76]. For masses below 5 GeV, they are primarily produced in the decay of B-hadrons along with a charged lepton, but the lepton p_T is too small to be recorded by conventional pp triggers, making more than 99 % of the events unobservable. As a result, the observable number of events per running time in PbPb with low-p_T triggers is comparable to that in pp collisions with conventional triggers. If lighter nuclei are used, allowing for higher luminosities (Table 2), then HI collisions can even yield a larger number of observable LLP events than pp (Fig. 2, right) [71].

5.2 Dark photons

The dark photon A' is an hypothetical extra-U(1) gauge boson that acts as a messenger particle between a dark sector, constituted of DM particles, that couples with a residual interaction g to the Standard Model particles. If the dark photon is the lightest state of the dark sector it can only decay into SM particles. Typical experimental searches focus on A' decays to dielectrons (if $m_{A'} < 2m_\mu$), dimuons (for masses above twice the muon mass) or dihadrons, and have so far constrained its existence in the mixing parameter g^2 versus mass $m_{A'}$ plane. Collider experiments search for the $A' \to \ell$ in Dalitz meson decays $\pi^0, \eta, \eta' \to \gamma A'$, meson decays $K \to \pi A'$, $\phi \to \eta A'$, and $D^* \to D^0 A'$, radiative decay of vector resonances $\upsilon(3S)$ decays in BaBar, and $\phi \to e^+e^-$ in KLOE in e^+e^- collisions [13]. HI experiments often feature excellent capabilities for electron and muon identification at low transverse momenta, and for vertexing, leading to competitive searches of low-mass A' from large samples of meson Dalitz decays. As an example of HI feasibility, ALICE is expected to reach a limit in g of about 10^{-4} at 90 % CL for A' masses 20–90 MeV with pp, pPb and PbPb collisions in Run-3 [13]. Such limits may eventually be superseded by LHCb and fixed-target experiments [77], although any increase in the total HI integrated luminosities, e.g. running with lighter ions as advocated here, can render the former competitive.

6 Thermal processes

6.1 Sexaquarks

The sexaquark S is a hypothesized neutral stable dibaryon $uuddss$ system, that can account for DM in the universe. The S would likely have a mass in the range $m_S \approx 2m_p \pm m_\pi$, and would have escaped detection to date [78]. Being a flavour singlet, the lightest particle to which it could be significantly coupled is the flavour singlet superposition of ω–ϕ, leading to an estimated size of $r_S = 0.1$–0.2 fm [79]. If a stable sexaquark exists, it is an attractive DM candidate because the sexaquark-to-baryon density ratio can be predicted by simple statistical arguments in the QGP-hadronization transition with known QCD parameters (quark masses and $T_{\rm QCD}$) to be $\approx 4.5 \pm 1$, in agreement with the observed DM-to-baryon ratio $\Omega_{\rm DM}/\Omega_b = 5.3 \pm 0.1$. This ratio is not modified during the subsequent universe expansion as long as $r_S \lesssim 0.2$ fm [79], thereby evading the counter-arguments against dibaryon DM given in [80–82].

If a stable or weakly-decaying dibaryon exists, its production in HI collisions can be completely predicted as a function of its mass, the temperature T, and the local baryon chemical potential μ_b of the produced QGP. A rough estimate for the central rapidity region, assuming $m_S = 2m_p$, $T = 150\,\text{MeV}$, and $\mu_b = 0$, gives $\{\pi : n : S\} \approx \{1 : 0.01 : 10^{-4}\}$. If the entire rapidity range were to come into thermal equilibrium, so the excess baryon number B of the initial ions is uniformly distributed in rapidity over the final state, in analogy with early universe conditions, it would imply $N_S - N_{\bar{S}} = \Omega_{\text{DM}}/\Omega_b(m_p/m_S)(N_B - N_{\bar{B}})$. Measuring the dependence of S and $\bar{S}$ production on $\sqrt{s_{\text{NN}}}$, colliding species, and rapidity would be very revealing and could directly connect DM production in HI collisions to that in the early universe.

Demonstrating that S and $\bar{S}$ are produced and measuring their production rates is difficult due to the vastly greater abundance of (anti)neutrons with similar mass to m_S and larger scattering and annihilation cross sections in the detector. Studies are underway to understand the accuracy with which different techniques can identify the production of S and $\bar{S}$, either exploiting the excellent hadron-identification capability over a wide momentum range in ALICE and LHCb, or the larger acceptance of the multi-purpose ATLAS and CMS detectors. Three basic approaches are being considered [78]:

- S particles produced in the primary collision can annihilate with a nucleon in the tracker material and produce a final state with $B = -1$, $S = +2$. LHC detectors can search for $\bar{S}p \to K^+\bar{\Lambda}^0$ or $\bar{S}n \to K^0\bar{\Lambda}^0$. The $\bar{\Lambda}^0$ is readily identified; in the absence of an $\bar{S}$, $\bar{\Lambda}^0$ production is only consistent with baryon number conservation if the collision is initiated by an anti-baryon and the $\bar{\Lambda}^0$ is accompanied by a baryon. Due to the significant penalty for producing a 2-body final state, the rate could be several orders of magnitude greater if the analysis could be extended to events with > 2 final particles coming from the vertex.
- Given the $\mathcal{O}(10^{-2})$ production rate of S or $\bar{S}$ relative to single baryons, there may be comparable numbers of events with an $S\bar{S}$ pair or with just a single S or $\bar{S}$ produced, with B and strangeness numbers balanced by two (anti-)baryons and 0–2 kaons. It may be possible to establish a systematic correlation of missing $\Delta B = \mp 2$; $\Delta S = \pm 2$ on a statistical basis.
- A population of neutral interacting and/or annihilating particles, distinct from n and $\bar{n}$ by virtue of having different scattering and annihilation cross sections (and different final states, if that is incorporated into the analysis), is in principle discernible by plotting the rate of such reactions as a function of the tracker material grammage and searching for additional exponential components.

6.2 Magnetic monopoles

For central collisions in which a thermal fireball is created, magnetic monopoles may, in principle, be created thermally. Although their microphysical cross sections are not known due to the strong coupling of magnetic monopoles, it seems reasonable to assume that there would exist some production mechanism in a thermal bath containing particles that couple to them (such as photons). Thus, if a temperature T is reached in a given HI collision, one would expect to produce monopoles with masses $m \lesssim T$, and an order of magnitude or so heavier when integrated over the luminosity. Studies based on this production channel would provide an approach to monopole searches independent from, and complementary to, that of production by strong fields (Section 4.1). However, at LHC energies one would expect production by strong fields to dominate as $T^2 \sim 0.3\,\text{GeV}^2 \ll g\text{B} \sim 100\,\text{GeV}^2$, where $g = 2\pi/e$ is the minimum magnetic charge [46] and B is the magnetic field produced in a typical UPC [67]. The experimental signatures would be as for Section 4.1, except that in this case more central HI collisions are favoured.

7 Summary

The scientific case of exploiting heavy-ion (HI) collisions at the LHC in searches for physics beyond the Standard Model (BSM) has been summarized. A non-comprehensive but representative list of BSM processes accessible with HI at the LHC has been presented based on four underlying mechanisms of production: $\gamma\gamma$ fusion in ultraperipheral collisions, "Schwinger" production through strong classical EM fields, hard scattering processes, and thermal production in the quark-gluon-plasma (QGP). Such searches provide additional motivations, beyond the traditional QGP physics programme, to prolong the HI runs past their currently scheduled end in 2029 (Run-4). Despite the lower nucleus-nucleus c.m. energies and

beam luminosities compared to pp collisions, HI are more competitive than the latter in particular BSM scenarios, whereas in some others they can complement or confirm searches (or discoveries) performed in the pp mode. Ultraperipheral collisions (UPC) of ions offer, in particular, a unique way to exploit the LHC as an intense $\gamma\gamma$ collider, profiting from the Z^4 enhancement factor in their cross sections, providing a clean and well understood environment within which to search for BSM states with QED couplings at masses $m_X \lessapprox 100\,\text{GeV}$ that are otherwise impossible in the pp mode. The UPC discovery potential for new particles, such as axion-like pseudoscalar or radions, and/or new interactions, such as non-linear Born-Infeld or non-commutative QED interactions, is unrivaled in this mass range. For magnetic monopoles, the huge electromagnetic fields present in HI lead to exponential enhancements of their cross sections and allow for first-principles calculations that are otherwise hindered in similar pp analyses. Central HI collisions provide also a propitious environment for searching for a possible stable sexaquark (QCD dark matter candidate). In the case of BSM signals produced through hard scatterings, the absence of pileup, the improved primary and displaced vertexing, and the lower trigger thresholds of HI compared to pp collisions, provide superior conditions for searches for BSM long-lived particles (LLPs) at low masses: An illustrative case has been made based on right-handed neutrinos with $m_\nu \lesssim 5\,\text{GeV}$. The improved particle identification capabilities and lower p_T thresholds of the ALICE and LHCb experiments make them also competitive detectors for dark-photon searches. Both LLPs and dark photon searches would benefit from the increased nucleon-nucleon luminosity accessible in collisions with light- and intermediate-ion species. Extrapolations based on the current LHC performance indicate that nucleon-nucleon integrated luminosities in the fb^{-1} range per month can be easily achieved with lighter ions after the Run-4.

References

[1] J. Coupard et al. (2016). №: CERN-ACC-2016-0041.
[2] S. R. Klein. *Nucl. Instrum. Meth.* A459 (2001). DOI: 10.1016/S0168-9002(00)00995-5.
[3] J. M. Jowett et al. 2004. №: EPAC-2004-MOPLT020, CERN-LHC-PROJECT-REPORT-772.
[4] R. Bruce et al. *Phys. Rev. Lett.* 99 (2007). DOI: 10.1103/PhysRevLett.99.144801.
[5] R. Bruce et al. *Phys. Rev. Accel. Beams* 12 (2009). DOI: 10.1103/PhysRevSTAB.12.071002.
[6] M. Schaumann. 2015. №: CERN-THESIS-2015-195, URN:NBN:DE:HBZ:82-RWTH-2015-050284.
[7] H.-H. Braun et al. 2004. №: EPAC-2004-MOPLT010.
[8] P. Hermes et al. 2016. №: CERN-THESIS-2016-230.
[9] P. Hermes et al. *Nucl. Instrum. Meth.* A819 (2016). DOI: 10.1016/j.nima.2016.02.050.
[10] R. Bruce et al. 2014. DOI: 10.18429/JACoW-IPAC2014-MOPRO042.
[11] A. Lechner et al. DOI: 10.18429/JACoW-IPAC2014-MOPRO021.
[12] G. Apollinari et al. (2017). DOI: 10.23731/CYRM-2017-004.
[13] Z. Citron et al. (2018). arXiv: 1812.06772 [hep-ph].
[14] J. Jowett. CERN. 2018. URL: https://indico.cern.ch/event/686494/timetable.
[15] M. Schaumann et al. 2018. DOI: 10.18429/JACoW-IPAC2018-MOPMF039.
[16] V. M. Budnev et al. *Phys. Rept.* 15 (1975). DOI: 10.1016/0370-1573(75)90009-5.
[17] A. J. Baltz et al. *Phys. Rept.* 458 (2008). DOI: 10.1016/j.physrep.2007.12.001.
[18] L. A. Harland-Lang et al. (2018). arXiv: 1810.06567 [hep-ph].
[19] S. Knapen et al. *Phys. Rev. Lett.* 118 (2017). DOI: 10.1103/PhysRevLett.118.171801.
[20] **CMS** (2018). arXiv: 1810.04602 [hep-ex].
[21] **LHC Forward Physics**. *J. Phys.* G43 (2016). DOI: 10.1088/0954-3899/43/11/110201.
[22] **ATLAS** (2015). №: CERN-LHCC-2015-009, ATLAS-TDR-024.
[23] **CMS, TOTEM** (2014). №: CERN-LHCC-2014-021, TOTEM-TDR-003, CMS-TDR-13.
[24] **FP420 R&D**. *JINST* 4 (2009). DOI: 10.1088/1748-0221/4/10/T10001.
[25] S. R. Klein et al. *Comput. Phys. Commun.* 212 (2017). DOI: 10.1016/j.cpc.2016.10.016.
[26] R. D. Peccei et al. *Phys. Rev. Lett.* 38 (1977). DOI: 10.1103/PhysRevLett.38.1440.
[27] F. Wilczek. *Phys. Rev. Lett.* 40 (1978). DOI: 10.1103/PhysRevLett.40.279.
[28] D. d'Enterria et al. *Phys. Rev. Lett.* 111 (2013). DOI: 10.1103/PhysRevLett.111.080405.
[29] **ATLAS**. *Nature Phys.* 13 (2017). DOI: 10.1038/nphys4208.

[30] S. Knapen et al. (2017). arXiv: 1709.07110 [hep-ph].
[31] M. J. Dolan et al. *JHEP* 12 (2017). DOI: 10.1007/JHEP12(2017)094.
[32] M. Born et al. *Proc. Roy. Soc. Lond.* A144 (1934). DOI: 10.1098/rspa.1934.0059.
[33] E. S. Fradkin et al. *Phys. Lett.* 163B (1985). DOI: 10.1016/0370-2693(85)90205-9.
[34] J. Ellis et al. *Phys. Rev. Lett.* 118 (2017). DOI: 10.1103/PhysRevLett.118.261802.
[35] J. Gomis et al. *JHEP* 08 (2000). DOI: 10.1088/1126-6708/2000/08/011.
[36] J. L. Hewett et al. *Phys. Rev.* D64 (2001). DOI: 10.1103/PhysRevD.64.075012.
[37] F. Richard (2017). arXiv: 1712.06410 [hep-ex].
[38] K.-m. Cheung. *Phys. Rev.* D61 (2000). DOI: 10.1103/PhysRevD.61.015005.
[39] H. Davoudiasl. *Phys. Rev.* D60 (1999). DOI: 10.1103/PhysRevD.60.084022.
[40] O. Cakir et al. *Eur. Phys. J.* C56 (2008). DOI: 10.1140/epjc/s10052-008-0658-7.
[41] B. Grinstein et al. *Phys. Lett.* B662 (2008). DOI: 10.1016/j.physletb.2008.03.020.
[42] A. Delgado et al. *Phys. Rev.* D81 (2010). DOI: 10.1103/PhysRevD.81.056003.
[43] S. Kathrein et al. *Phys. Rev.* D84 (2011). DOI: 10.1103/PhysRevD.84.015010.
[44] L. Beresford et al. (2018). arXiv: 1811.06465 [hep-ph].
[45] L. A. Harland-Lang et al. (2018). arXiv: 1812.04886 [hep-ph].
[46] P. A. M. Dirac. *Proc. Roy. Soc. Lond.* A133 (1931). DOI: 10.1098/rspa.1931.0130.
[47] Yu. Kurochkin et al. *Mod. Phys. Lett.* A21 (2006). DOI: 10.1142/S0217732306022237.
[48] L. N. Epele et al. *Eur. Phys. J. Plus* 127 (2012). DOI: 10.1140/epjp/i2012-12060-8.
[49] J. T. Reis et al. *Phys. Rev.* D96 (2017). DOI: 10.1103/PhysRevD.96.075031.
[50] S. Baines et al. *Eur. Phys. J.* C78 (2018). DOI: 10.1140/epjc/s10052-018-6440-6.
[51] H. Fanchiotti et al. *Int. J. Mod. Phys.* A32 (2017). DOI: 10.1142/S0217751X17502025.
[52] I. F. Ginzburg et al. *Sov. J. Nucl. Phys.* 36 (1982). №: IAEM-82-185.
[53] I. F. Ginzburg et al. *Phys. Rev.* D57 (1998). DOI: 10.1103/PhysRevD.57.R6599.
[54] **D0**. *Phys. Rev. Lett.* 81 (1998). DOI: 10.1103/PhysRevLett.81.524.
[55] L. P. Gamberg et al. *Found. Phys.* 30 (2000). DOI: 10.1023/A:1003668812097.
[56] K. A. Milton. *Rept. Prog. Phys.* 69 (2006). DOI: 10.1088/0034-4885/69/6/R02.
[57] J. Preskill. *Ann. Rev. Nucl. Part. Sci.* 34 (1984). DOI: 10.1146/annurev.ns.34.120184.002333.
[58] J. Polchinski. *Int. J. Mod. Phys.* A19S1 (2004). DOI: 10.1142/S0217751X0401866X.
[59] **Particle Data Group**. *Phys. Rev.* D98 (2018). DOI: 10.1103/PhysRevD.98.030001.
[60] **MoEDAL**. *Phys. Lett.* B782 (2018). DOI: 10.1016/j.physletb.2018.05.069.
[61] G. 't Hooft. *Nucl. Phys.* B79 (1974). DOI: 10.1016/0550-3213(74)90486-6.
[62] A. M. Polyakov. *JETP Lett.* 20 (1974). №: PRINT-74-1566 (LANDAU-INST).
[63] E. Witten. *Nucl. Phys.* B160 (1979). DOI: 10.1016/0550-3213(79)90232-3.
[64] A. K. Drukier et al. *Phys. Rev. Lett.* 49 (1982). DOI: 10.1103/PhysRevLett.49.102.
[65] C. Papageorgakis et al. *JHEP* 09 (2014). DOI: 10.1007/JHEP09(2014)128.
[66] C. J. Goebel. University of Chicago Press, 1970. ISBN: 9780226262802.
[67] X.-G. Huang. *Rept. Prog. Phys.* 79 (2016). DOI: 10.1088/0034-4885/79/7/076302.
[68] I. K. Affleck et al. *Nucl. Phys.* B194 (1982). DOI: 10.1016/0550-3213(82)90511-9.
[69] Y. D. He. *Phys. Rev. Lett.* 79 (1997). DOI: 10.1103/PhysRevLett.79.3134.
[70] O. Gould et al. *Phys. Rev. Lett.* 119 (2017). DOI: 10.1103/PhysRevLett.119.241601.
[71] M. Drewes et al. (2018). arXiv: 1810.09400 [hep-ph].
[72] D. Curtin et al. (2018). arXiv: 1806.07396 [hep-ph].
[73] G. Apollinari et al. (2015). DOI: 10.5170/CERN-2015-005.
[74] G. Apollinari et al. *CERN Yellow Report* (2015). DOI: 10.5170/CERN-2015-005.1.
[75] **CMS**. *Phys. Rev. Lett.* 119 (2017). DOI: 10.1103/PhysRevLett.119.242001.
[76] T. Asaka et al. *Phys. Lett.* B620 (2005). DOI: 10.1016/j.physletb.2005.06.020.
[77] P. Ilten et al. *Phys. Rev. Lett.* 116 (2016). DOI: 10.1103/PhysRevLett.116.251803.
[78] G. R. Farrar (2017). arXiv: 1708.08951 [hep-ph].
[79] G. R. Farrar (2018). arXiv: 1805.03723 [hep-ph].
[80] C. Gross et al. *Phys. Rev.* D98 (2018). DOI: 10.1103/PhysRevD.98.063005.
[81] S. D. McDermott et al. (2018). arXiv: 1809.06765 [hep-ph].
[82] E. W. Kolb et al. (2018). arXiv: 1809.06003 [hep-ph].